Biophysical Journal Volume 69 November 1995 1734–1747

Modeling the Effect of Glutamate Diffusion and Uptake on NMDA and Non-NMDA Receptor Saturation

William R. Holmes
Neurobiology Program, Department of Biological Sciences and College of Osteopathic Medicine, Ohio University, Athens, Ohio 45701-2979, USA

ABSTRACT One- and two-dimensional models of glutamate diffusion, uptake, and binding in the synaptic cleft were developed to determine if the release of single vesicles of glutamate would saturate NMDA and non-NMDA receptors. Ranges of parameter values were used in the simulations to determine the conditions when saturation could occur. Single vesicles of glutamate did not saturate NMDA receptors unless diffusion was very slow and the number of glutamate molecules in a vesicle was large. However, the release of eight vesicles at 400 Hz caused NMDA receptor saturation for all parameter values tested. Glutamate uptake was found to reduce NMDA receptor saturation, but the effect was smaller than that of changes in the diffusion coefficient or in the number of glutamate molecules in a vesicle. Non-NMDA receptors were not saturated unless diffusion was very slow and the number of glutamate molecules in a vesicle was large. The release of eight vesicles at 400 Hz caused significant non-NMDA receptor desensitization. The results suggest that NMDA and non-NMDA receptors are not saturated by single vesicles of glutamate under usual conditions, and that tetanic input, of the type typically used to induce long-term potentiation, will increase calcium influx by increasing receptor binding as well as by reducing voltage-dependent block of NMDA receptors.

INTRODUCTION

Calcium influx through NMDA receptor channels has been shown to be necessary for the induction of long-term potentiation (LTP) and long-term depression (LTD) (for a review, see Baudry and Davis, 1991, 1994). It has been proposed that whether a synapse undergoes LTP or LTD depends on the magnitude of the calcium concentration change at the synapse (Lisman, 1989; Holmes and Levy, 1990). High-frequency tetanic stimulation of the type used to induce LTP may enhance calcium influx through NMDA receptor channels by two mechanisms: 1) by relieving voltage-dependent magnesium block of the channels, and 2) by having glutamate bind to additional receptors or receptor binding sites with each pulse in the stimulus train. Although the voltage dependence of magnesium block of the NMDA receptor channel has been well described, it is not known if subsequent pulses in a tetanus actually cause additional glutamate binding to NMDA receptors.

Recent reports suggest that a single vesicle of glutamate may saturate NMDA (Clements et al., 1992) and non-NMDA (Tang et al., 1994) receptors at hippocampal synapses. If NMDA receptors are saturated by a single vesicle of glutamate, then subsequent pulses in a high-frequency stimulus train would fail to increase the peak number of open NMDA receptor channels by recruiting additional receptors; the only role of the tetanus would be to relieve magnesium block. In previous modeling work (Holmes and Levy, 1990, and unpublished calculations), we found that predictions of the amount of calcium entry through NMDA receptor channels were strongly influenced by whether the peak number of bound NMDA receptors was allowed to increase during a tetanus. If NMDA receptors are saturated by a single vesicle of glutamate, then the increase in calcium influx due to the tetanus would be limited, and calcium levels that lead to LTP would be hard to distinguish from those that lead to LTD.

The goal of this study was to determine if the release of a single vesicle of glutamate or the tetanic release of eight vesicles of glutamate at 400 Hz could saturate NMDA and non-NMDA receptors. Diffusion models of the synaptic cleft and the volume outside the cleft were constructed, and the equations were solved for ranges of parameter values. Percentage saturation was defined as the maximum percentage of receptors, at any given time during the simulation, that had both of their binding sites occupied by glutamate. Receptors were considered to be saturated if the percentage saturation exceeded 90%. It was found that the extent of NMDA receptor saturation depends strongly on assumptions about the number of glutamate molecules in a vesicle and the glutamate diffusion coefficient, and on glutamate uptake. For the parameter values thought to be most consistent with experimental data, NMDA receptors did not saturate with a single vesicle of glutamate, but did saturate with the eight pulse tetanus. Non-NMDA receptors also did not saturate with a single vesicle of glutamate, and an eight-pulse tetanus caused significant receptor desensitization.

Received for publication 13 April 1995 and in final form 10 August 1995.

Address reprint requests to Dr. William R. Holmes, Neurobiology Program Department of Biological Sciences, Ohio University, Athens, OH 45701-2979. Tel.: 614-593-0075; Fax: 614-593-0300; E-mail: wholmes1@ohiou.edu.

0006-3495/95/11/1734/00 $2.00

METHODS

Representation of the synaptic cleft

The synaptic cleft was modeled as a flat cylinder (Fig. 1). Vesicular release of glutamate was assumed to occur over a radius v from the center of the top surface of the cylinder. NMDA and non-NMDA receptors were located within a radius n from the center of the bottom surface of the cylinder. There were two types of glutamate uptake transporters modeled. Uptake into the presynaptic neuron was assumed to occur between radii v and u at the top surface of the cylinder, and uptake into glia was assumed to occur beyond radius u, also at the top surface of the cylinder. Any glutamate that managed to diffuse as far as the lateral surface of the cylinder was assumed to be taken up, i.e., the concentration of glutamate at the lateral surface of the cylinder was zero.

Mathematical procedure

Two-dimensional model

The three-dimensional diffusion equation in cylindrical coordinates (r, z, θ) was reduced to the two-dimensional equation in (r, z) by assuming symmetry in the angular variable θ.

$$\frac{\partial A}{\partial t} = D\left\{\frac{1}{r}\frac{\partial A}{\partial r} + \frac{\partial^2 A}{\partial r^2} + \frac{\partial^2 A}{\partial z^2}\right\} \tag{1}$$

The variable r represents the radial dimension from the center of the cleft into the extracellular space, and the variable z represents the dimension across the synaptic cleft from the presynaptic to the postsynaptic neuron. In this equation A is glutamate concentration and D is the diffusion coefficient for glutamate. A grid in r and z was constructed, and this equation was solved using the alternating direction implicit method (ADI method) (e.g., Gerald and Wheatley, 1994). A grid size of 0.5 nm for Δr and Δz was used most often. The Δt was 0.05–0.2 μs for most simulations (the smaller value was used with high uptake capacity and large numbers of glutamate molecules in a vesicle) but was 0.01 μs when looking at changes across the cleft (z axis) over the first 20 μs after release.

Uptake was incorporated by adding a Michaelis-Menten term to Eq. 1 for grid points along the top surface as follows:

$$\frac{\partial A}{\partial t} = D\left\{\frac{1}{r}\frac{\partial A}{\partial r} + \frac{\partial^2 A}{\partial r^2} + \frac{\partial^2 A}{\partial z^2}\right\} - \frac{V_{max}(i)A}{A + K_m(i)} \tag{2}$$

where the index i distinguishes between neuronal, glial, or no uptake.

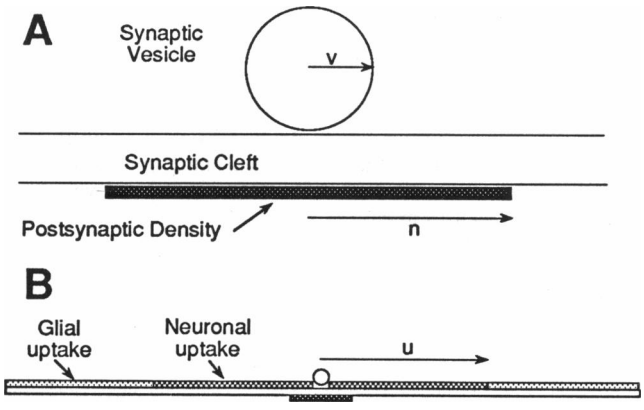

FIGURE 1 Representation of the synaptic cleft. (*A*) The radius v of the synaptic vesicle was 0.025 μm, the cleft was 0.02 μm wide, and the postsynaptic density was circular with a radius of 0.1 μm. (*B*) More global view showing the areas of neuronal and glial glutamate uptake. Radius u was 0.5 μm.

At the bottom surface glutamate binds to NMDA and non-NMDA receptors. Binding to NMDA receptors was modeled according to the following kinetic scheme:

$$A + R \underset{k_{off}}{\overset{2k_{on}}{\rightleftharpoons}} AR + A \underset{2k_{off}}{\overset{k_{on}}{\rightleftharpoons}} A_2R \underset{\alpha}{\overset{\beta}{\rightleftharpoons}} A_2R^*$$

$$A_2D$$

where A (agonist) is free glutamate, R is free receptor, and AR, A_2R, A_2D, and A_2R^* represent the single bound, double bound, desensitized, and open states of the receptor-agonist complex. Although most proposed kinetic schemes allow entry into the desensitized state only from the double bound state (Clements and Westbrook, 1991; Lester and Jahr, 1992), there is evidence to suggest that the desensitized state can be entered from the open state as well (Lin and Stevens, 1994).

This set of kinetic equations yields the following differential equations:

$$\begin{aligned}
\frac{dA_2R^*}{dt} &= -(\alpha + k_{d2})A_2R^* + \beta A_2R + k_{r2} A_2D \\
\frac{dA_2D}{dt} &= -(k_{r1} + k_{r2})A_2D + k_{d1} A_2R + k_{d2} A_2R^* \\
\frac{dA_2R}{dt} &= -(\beta + k_{d1} + 2k_{off})A_2R + \alpha A_2R^* \\
&\quad + k_{r1} A_2D + (k_{on} A)AR \\
\frac{dAR}{dt} &= -(k_{on} A + k_{off})AR + (2k_{on} A)R + 2k_{off} A_2R \\
\frac{dA}{dt} &= -(2k_{on} R + k_{on} AR)A + k_{off} AR + 2k_{off} A_2R
\end{aligned} \tag{3}$$

Binding to non-NMDA receptors was modeled with the kinetic scheme proposed by Jonas et al. (1993). This scheme was chosen because it was developed for hippocampal non-NMDA receptors and it allows desensitization from the single bound state as well as from the double bound and open states. This scheme was

$$\begin{array}{ccccccc}
A + R & \underset{k_{off1}}{\overset{k_{on1}}{\rightleftharpoons}} & AR + A & \underset{k_{off2}}{\overset{k_{on2}}{\rightleftharpoons}} & A_2R & \underset{\alpha}{\overset{\beta}{\rightleftharpoons}} & A_2R^* \\
 & & \alpha_1 \uparrow\downarrow \beta_1 & & \alpha_2 \uparrow\downarrow \beta_2 & & \alpha_3 \uparrow\downarrow \beta_3 \\
 & & AD + A & \underset{k_{off3}}{\overset{k_{on3}}{\rightleftharpoons}} & A_2D & \underset{\alpha_4}{\overset{\beta_4}{\rightleftharpoons}} & A_2D^*
\end{array}$$

Two other kinetic schemes were tested. One was identical to that described above for the NMDA receptors, but it was abandoned because it did not include the important single bound desensitized state. The other was the scheme proposed by Raman and Trussell (1992, 1995) for embryonic chick nucleus magnocellularis neurons. Because hippocampal receptors were of interest for this study, the data plotted in the figures were computed with the Jonas et al. (1993) scheme.

This non-NMDA binding reaction scheme can be modeled by a set of seven differential equations entirely analogous to Eq. 3.

To solve Eq. 1 in conjunction with the auxiliary equations Eq. 3, it was assumed that glutamate concentration was constant over the time step of integration of Eq. 3. This assumption eliminated the last of the equations in Eq. 3 and made the remaining equations linear. Being linear, they could be solved simply with an improved Euler method. The change in glutamate at

the bottom surface due to binding was incorporated into Eq. 1 for the grid points representing the bottom surface as

$$\frac{\partial A}{\partial t} = D\left\{\frac{1}{r}\frac{\partial A}{\partial r} + \frac{\partial^2 A}{\partial z^2} + \frac{\partial^2 A}{\partial z^2}\right\} + \{-(2k_{on}A)R + k_{off}AR - (k_{on}A)AR + 2k_{off}A_2R\}_{NMDA} \quad (4)$$
$$+ \{-(k_{on_1}A)R + k_{off_1}AR - (k_{on_2}A)AR + k_{off_2}A_2R - (k_{on_3}A)AD + k_{off_3}A_2D\}_{AMPA}$$

where the subscripts NMDA and AMPA indicate terms for NMDA and non-NMDA receptor binding, respectively.

The numerical procedure was as follows:

1. Use the glutamate concentration at time t to solve the equations for the NMDA and non-NMDA binding reaction states at $t + \Delta t/4$ (i.e., for A fixed at its value at time t, solve Eq. 3 for AR, A_2R, A_2D, and A_2R^* for the NMDA reaction and an analogous set of equations for AR, A_2R, AD, A_2D, A_2D^*, and A_2R^* for the non-NMDA reaction at $t + \Delta t/4$).
2. Use the receptor state values at $t + \Delta t/4$ to solve Eqs. 1, 2, and 4 for glutamate concentration at $t + \Delta t/2$ by sweeping through the r dimension (first half of the ADI method).
3. Use the glutamate concentration at $t + \Delta t/2$ to solve the equations for the NMDA and non-NMDA binding reaction states at $t + 3\Delta t/4$.
4. Use the receptor state values at $t + 3\Delta t/4$ to finish the ADI computation by sweeping through the z dimension to get glutamate concentration at $t + \Delta t$.

Solving the auxiliary equations at half time steps with respect to the partial differential equation in this manner is a procedure recommended for use with the equations of nerve conduction (Mascagni, 1989).

One-dimensional approximation

Because the z dimension (height of the synaptic cleft) is small compared to the radial extent of the volume being modeled, Eqs. 1, 2, and 4 above for glutamate concentration might be approximated by eliminating the terms in z and by appending the additional terms found in Eqs. 2 and 4 to Eq. 1. When this was done, the resulting equation and auxiliary equations were similar to those used by Wathey et al. (1979) in models of the neuromuscular junction. The one-dimensional approximation was used to check the accuracy of the numerical procedure by comparing results with specific cases reported by Wathey et al. (1979).

Initial conditions and boundary conditions

The release of neurotransmitter was modeled as in Wathey et al. (1979). That is, initial transmitter concentration was zero except that

$$A(r, 0, 0) = \alpha[(r/v)^4 - 2(r/v)^2 + 1] \quad 0 \le r \le v$$

where v is the vesicle radius and α is a constant that converts the number of transmitter molecules into a concentration. Initial values of all other variables were set to 0. Boundary conditions were sealed ends at the top and bottom ($\partial A/\partial z = 0$) and zero glutamate concentration at the lateral boundary.

Parameter value ranges used in the simulations

The model required values for numerous parameters. The ranges of values used are given in Table 1. Simulations used the values in the middle column of Table 1 unless stated otherwise.

TABLE 1 Parameter values and ranges used in the simulations

Parameter	Symbol	Value	Range tested
Glutamate diffusion coeff.	D	0.25 μm^2/ms	0.1–0.4
PSD diameter		0.2 μm	
Glutamate molecules in a vesicle		3000	1000–10000
NMDA receptor density		600/μm^2	200–2000
Non-NMDA receptor density		3000/μm^2	1000–10000
Uptake affinity (neuron)	K_m	2 μM	2 μM (high) 20 μM (low)
Uptake affinity (glia)	K_m	200 μM	200 μM (high) 1 mM (low)
Uptake capacity (neuron)	V_{max}	80*	80, 400, 800
Uptake capacity (glia)	V_{max}	240*	240, 1200, 2400
Non-NDMA binding	k_{on1}	0.00918 μM^{-1} ms^{-1}	
	k_{off1}	8.52 ms^{-1}	
	k_{on2}	0.0568 μM^{-1} ms^{-1}	
	k_{off2}	6.52 ms^{-1}	
	k_{on3}	0.00254 μM^{-1} ms^{-1}	
	k_{off3}	0.0914 ms^{-1}	
	α	1.8 ms^{-1}	
	β	8.5 ms^{-1}	
	α_1	0.0784 ms^{-1}	
	β_1	5.78 ms^{-1}	
	α_2	001454 ms^{-1}	
	β_2	0.344 ms^{-1}	
	α_3	0.008 ms^{-1}	
	β_3	0.0354 ms^{-1}	
	α_4	0.3808 ms^{-1}	
	β_4	0.0336 ms^{-1}	
NMDA binding	k_{on}	0.005 μM^{-1} ms^{-1}	
	k_{off}	0.0067 ms^{-1}	
	α	0.20 ms^{-1}	
	β	0.06 ms^{-1}	
	k_{d1}	0.01 ms^{-1}	
	k_{d2}	0.01 ms^{-1}	
	k_{r1}	0.002 ms^{-1}	
	k_{r2}	0.002 ms^{-1}	

*One-dimensional model values. The two-dimensional model values vary according to the grid size in the z direction.

Diffusion coefficient

The diffusion coefficient for glutamate in aqueous solution has been estimated to be 0.76 μm^2/ms (Longsworth, 1953). It is thought that the diffusion coefficient in the synaptic cleft should be about a factor of 3 lower because of tortuosity (Rice et al., 1985; Nicholson and Phillips, 1981; Garthwaite, 1985). A diffusion coefficient of 0.25 μm^2/ms was used most commonly in the simulations, but results were computed with values ranging from 0.1 to 0.4 μm^2/ms.

Binding kinetics

There have been numerous studies describing the binding kinetics of glutamate with NMDA (Clements and Westbrook, 1991; Edmonds and Colquhoun, 1992; Lester et al., 1990, 1993; Lester and Jahr, 1992) and non-NMDA receptors (Jonas et al., 1993; Patneau et al., 1992; Raman and Trussell 1992, 1995; Vyklicky et al., 1991). The NMDA parameter values used in the simulations were chosen to lie within the range of reported values. The non-NMDA parameter values used were those given by Jonas et al. (1993), except that they were multiplied by 2 (to compensate for temperature). Some simulations were done with the uncompensated values

and still others used the kinetic scheme and values given by Raman and Trussell (1995). Values chosen are given in Table 1.

Synaptic contact area

The total number of receptors depends on the area in which receptors are present and the receptor density. The area occupied by receptors was assumed to be circular, with a diameter of 0.2 μm and a surface area of 0.0314 μm^2. This surface area value is near the mean of postsynaptic density (PSD) areas measured for non-concave PSDs in dentate granule cells (Desmond and Levy, 1986).

Glutamate molecules in a vesicle

The number of glutamate molecules in a vesicle has been estimated to be 1000–5000 (Burger et al., 1989; Riveros et al., 1986). This is smaller than the number of acetylcholine molecules thought to be in a vesicle at the neuromuscular junction. The range of values simulated was 1000–10,000.

Receptor density

The density of non-NMDA and NMDA receptors at a synapse has not been measured. Rough estimates can be made based on the density of "particles" observed in freeze fracture studies (Harris and Landis, 1986). These studies indicate that there are 2000–4000 particles/μm^2 at a synapse. Acetylcholine receptor density at the neuromuscular junction is thought to be about 10,000/μm^2, but densities of receptors at hippocampal synapses are thought to be lower. An additional problem was to decide how many NMDA versus non-NMDA receptors should be modeled at a synapse. Given the fact that the single channel conductance of NMDA receptors is about 5 times larger than that for non-NMDA receptors, it was assumed initially that the densities should also differ by a factor of 5. Thus the range of densities tested was 200-2000/μm^2 for NMDA receptors and 1000–10,000/μm^2 for non-NMDA receptors. (With a PSD surface area of 0.0314 μm^2, a receptor density of 1000/μm^2 means that there are approximately 31 receptors.)

Glutamate uptake

Two different glutamate uptake systems have been identified in the brain (Balcar and Johnston, 1972a,b; Hertz et al., 1978; Hertz, 1979; Schousboe, 1981). One is a high-affinity system that is thought to mediate uptake into the presynaptic neuron. For example, uptake is very much reduced in the dentate following axotomy of perforant path neurons (Storm-Mathisen, 1977). The other is a lower-affinity system responsible for uptake into glia. Reported K_m values for the high- and low-affinity systems are 1–20 μM and 100-1000 μM, respectively. In the simulations the K_m value for the high-affinity system was either 2 or 20 μM, and the value for the low-affinity system was either 200 or 1000 μM. Reported V_{max} values were difficult to translate into model parameters, but reports suggest that the value for glial uptake is about 3 times that for neuronal uptake (Balcar and Johnston, 1972b), and this is the ratio used here. In the simulations the V_{max} can be interpreted as being the transport rate per transporter multiplied by the surface density of transporters multiplied by the surface-to-volume ratio. Values assumed for V_{max} in the one-dimensional model simulations were 80, 400, and 800 for neuronal uptake and 240, 1200, and 2400 for glial uptake. (Values in the two-dimensional model depended on the grid size in the z direction.) With a synaptic cleft width of 0.02 μm, a value of 80 could be interpreted to represent a transport rate of 1 glutamate molecule/ms with a transporter density of 1.6/μm^2 or a transport rate of 1 glutamate molecule/10 ms and a transporter density of 16/μm^2.

Estimating calcium influx

The number of open NMDA and non-NMDA channels as a function of time computed with the above model was used to determine synaptic conductances for use in a model of a dentate granule cell. This model has been fully described (Holmes and Levy, 1990). The somatic EPSPs due to activation of single synapses were computed with both NMDA and non-NMDA receptor mediated conductances present or with only the non-NMDA component present. Magnesium block of the NMDA receptor channel was included in the model with an assumed extracellular magnesium concentration of 1.2 mM. In this model synaptic conductances were activated at one or 108 synapses on dendritic spines either once or eight times at 400 Hz.

Calcium influx was computed from the calcium component of the current through the NMDA receptor channels, as in the previous dentate granule cell model. Comparisons of calcium influx during the 100-ms period after stimulation were made for the different conductances computed for the range of parameter values in Table 1.

RESULTS

Determining an appropriate lateral boundary condition

It was first necessary to determine the lateral extent of the extracellular space that should be included in the model. A usual assumption of this type of model is that neurotransmitter reaching the edge of the cleft is removed instantly from the system by uptake mechanisms. This assumption was not made here because uptake systems were explicitly included in the model. The lateral distance beyond the synaptic cleft that should be included in the model before the boundary condition of instant uptake is applied needed to be large enough that further increases in the lateral extent would not affect computed results, but small enough to limit computation time.

To determine an appropriate lateral extent for the model, the time course of glutamate in the cleft was modeled with the two-dimensional model, with a lateral extent of 0.1, 1.0, 4.0, and 8.0 μm. Three thousand glutamate molecules were released into the cleft either once at $t = 0$ or eight times at 400 Hz. To maximize differences among the four cases, no glutamate uptake was included. At the lateral boundary, uptake was instantaneous (i.e., glutamate concentration was zero).

As shown in Fig. 2, a lateral extent of 4 μm was appropriate for the model. Increasing the lateral extent to 8 μm produced negligible differences in glutamate decay, and hence negligible differences in non-NMDA and NMDA conductance time courses, whether for a single input or for a tetanus. The appropriateness of a lateral extent of 4 or 8 μm was confirmed by comparisons with the analytic solution for diffusion from an instantaneous point source in an infinite disk (Barbour et al., 1994). The curve computed with the analytic solution (not shown) entirely overlaps the curve for a lateral extent of 8 μm after the first 0.1 ms.

Conversely, lateral extents of 0.1 and 1.0 μm were clearly inappropriate. The boundary condition of instant uptake at the lateral boundary artificially drew glutamate out of the cleft much faster than it would leave by diffusion alone. With a lateral extent of 0.1 μm, almost no glutamate was left in the cleft after 100 μs. With a lateral extent of 1.0 μm, glutamate remained in the cleft a bit longer, but decay was

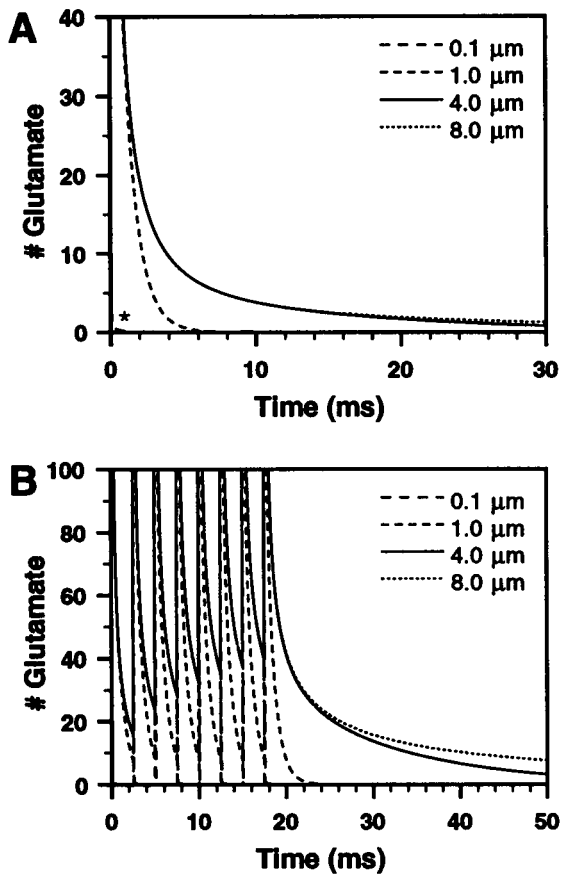

FIGURE 2 Glutamate molecules in the synaptic cleft for extracellular space extending 0.1, 1.0, 4.0, and 8.0 μm from the center of the cleft. Uptake was at the lateral boundary only. Although 3000 glutamate molecules were released, the graphs are scaled to 40 and 100 molecules to magnify differences in the simulations. D was 0.2 μm^2/ms and NMDA and non-NMDA receptor densities were 600 and 3000/μm^2, respectively. (*A*) Single vesicle release. The asterisk indicates that when the lateral boundary was 0.1 μm, the decay curve largely overlapped the graph axes. (*B*) Tetanic release of glutamate. The slight increase in glutamate with each pulse when the lateral extent was 4.0 or 8.0 μm did not occur when neuronal and glial uptake were included in the model. Decay was extremely rapid for a lateral boundary of 0.1 μm.

much faster than with lateral extents of 4.0 or 8.0 μm. This faster decay could bias studies of receptor saturation. Consequently, lateral extents of 4.0 μm or larger were used in the simulations. (When uptake was included in the model with a 4.0 μm lateral extent, the glutamate decay curve fell between those curves shown in Fig. 2 for lateral extents of 0.1 and 1.0 μm. See Fig. 5 below.)

Differences between one- and two-dimensional model results

Given that the lateral dimension of the model was much larger than the cleft height, it would seem that one- and two-dimensional models should yield identical results. If the lateral extent were 0.1 μm, then the lateral dimension would be only 5 times larger than the cleft height, and one- and two-dimensional models might produce different results. However, with a lateral extent of 4.0 μm, the lateral dimension was 200 times larger than the cleft height. To test whether differences between the one- and two-dimensional model results were negligible, the two-dimensional model was used to analyze differences in glutamate concentration across the height of the cleft (z dimension).

It was found, not surprisingly, that differences in glutamate concentration across the height of the cleft were negligible after the first 3 μs. This is similar to the result given by Eccles and Jaeger (1958). Glutamate concentrations were identical to three digits across the cleft by 2–3 μs, depending on the particular lateral distance being observed, and were identical to four digits by 9 μs. In models without uptake, differences in the third and fourth digit of glutamate concentration across the cleft began to reappear after 9 μs, presumably because of glutamate binding to receptors. In simulations with the highest level of glutamate uptake modeled, an equally small reverse gradient of glutamate concentration developed because of glutamate uptake into the presynaptic neuron. In all cases there was a significant gradient of glutamate concentration in the lateral direction (r direction), but a negligible gradient across the cleft (z direction).

Because results with one- and two-dimensional models were virtually identical, one-dimensional models were used to compute many of the results in the latter half of this paper.

Time course of glutamate in the cleft

The concentration of glutamate in the cleft will vary as a function of time depending on the distance from the release site, the glutamate diffusion coefficient, and the affinity and capacity of the glutamate uptake systems.

Fig. 3 shows the time course of glutamate at the postsynaptic membrane at different distances from the center of the postsynaptic density (PSD) or release site when uptake was included or not included in the model. Whether there was uptake or not, glutamate concentration at the center of the PSD was briefly at a level approaching that thought to exist in the synaptic vesicle (Burger et al., 1989; Riveros et al., 1986) or over 100 mM. At the edge of the cleft, or 0.1 μm from the center, peak glutamate concentration was 2.85 mM. Glutamate concentration above the PSD equilibrated by about 0.3 ms. Removing uptake had little effect on the peak concentration in the cleft, but it did affect the decay time course (compare Fig. 3, *B* and *C*). Although peak glutamate dropped substantially with distance (i.e., 100 μM at 0.5 μm from the center), all receptors experienced large glutamate concentrations because of the 0.1-μm radius of the PSD.

The diffusion coefficient of glutamate played a major role in determining the time course of glutamate in the cleft, as shown in Fig. 4. Here 3000 glutamate molecules were released into the synaptic cleft and the average concentra-

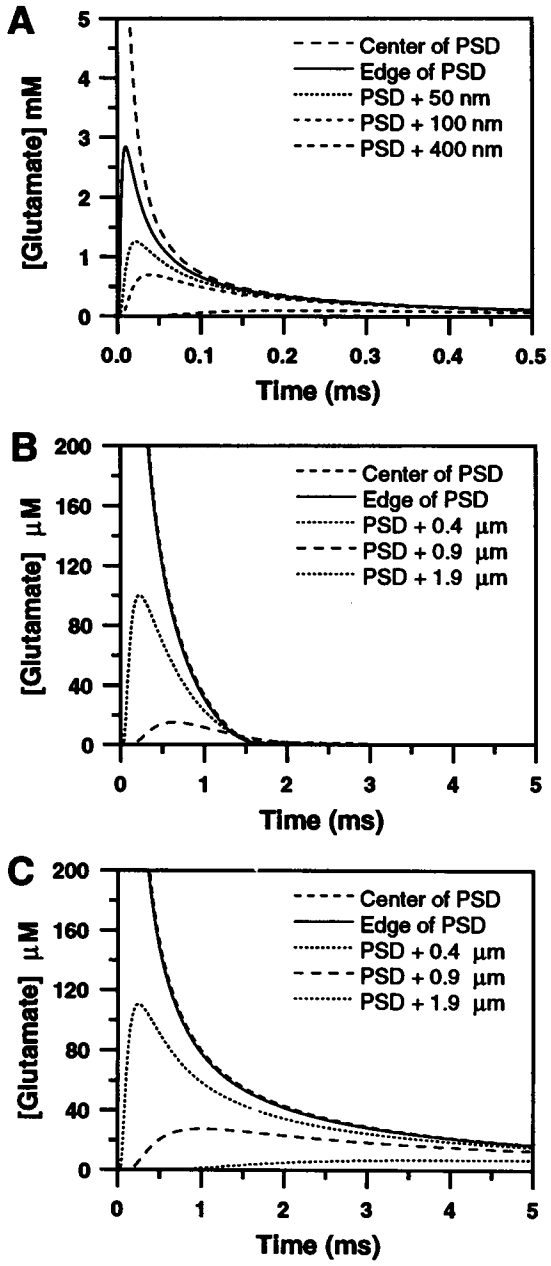

FIGURE 3 Time course of glutamate in the cleft. D was 0.25 μm^2/ms and the number of glutamate molecules released was 3000. Uptake affinities were 2 μM and 200 μM for neuronal and glial uptake, respectively. (*A*) Low uptake capacity; locations observed were in the first 0.5 μm from the center of the cleft. (*B*) Low uptake capacity, locations up to 2 μm from the cleft are shown. (The lines cross because of different uptake affinity and capacity beyond 0.5 μm.) (*C*) No uptake.

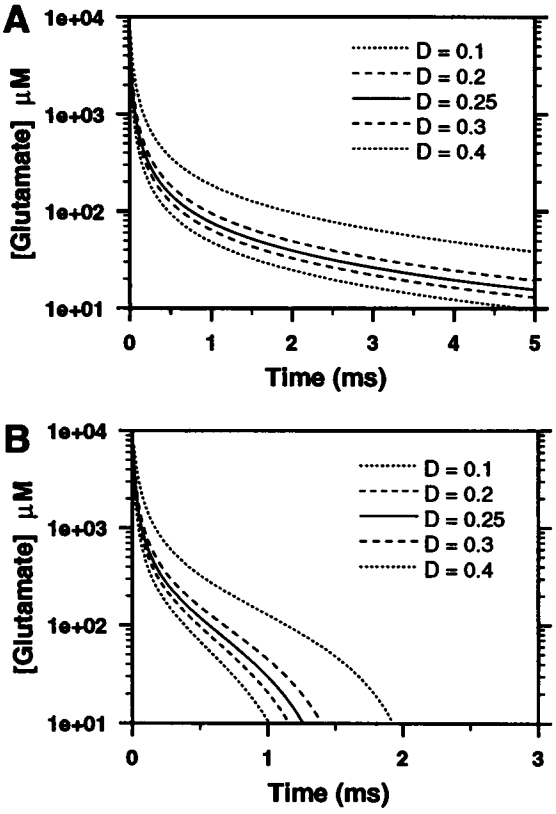

FIGURE 4 Effect of the glutamate diffusion coefficient on the time course of glutamate in the cleft. Three thousand glutamate molecules were released into the cleft. The concentration of glutamate averaged over the volume of the cleft is plotted on a log scale. One molecule in the cleft corresponds to a concentration less than 3 μM. (*A*) No uptake. (*B*) High affinity and low capacity uptake.

tion in the cleft is shown as a function of time for D = 0.1 to 0.4 μm^2/ms. Note that the largest difference in decay time course is seen between the D = 0.1 and D = 0.2 curves. If there were some factor besides tortuosity that could cause the glutamate diffusion coefficient to drop substantially, then the time course of glutamate in the synaptic cleft would be much prolonged.

Maximum uptake rate and to a lesser extent the affinity of glutamate for the glutamate transporters also played an important role in determining the time course of glutamate in the cleft, as shown in Fig. 5. Three different uptake capacities were modeled. As uptake capacity was increased, the time at which glutamate virtually disappeared from the cleft decreased from 1.5 ms to 0.6 ms to 0.35 ms. When the affinity constants for the two transporters were raised from 2 and 200 μM to 20 and 1000 μM, the decay time courses were not affected until the average glutamate concentration in the cleft was less than 150 μM. Below that number, decay was slowed and the times at which glutamate virtually disappeared from the cleft were $>$ 2.0 ms, 0.9 ms, and 0.5 ms for the three different uptake capacities.

Extent of NMDA and non-NMDA receptor saturation with single vesicles of glutamate

The extent of NMDA and non-NMDA saturation by single vesicles of glutamate was explored while varying the diffusion coefficient, the uptake affinity and capacity, the number of glutamate molecules in a vesicle, and receptor density. Percentage saturation was defined as the maximum over time of the percentage of receptors that had two glu-

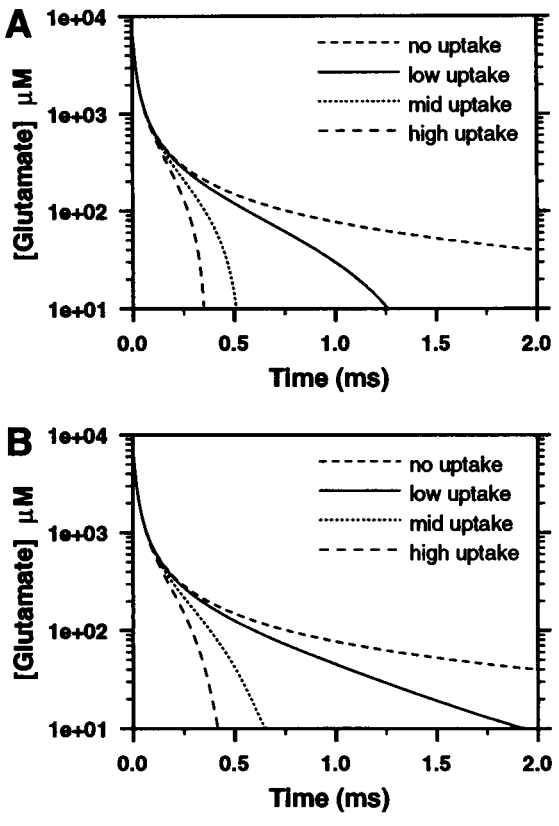

FIGURE 5 Effect of uptake affinity and capacity on the time course of glutamate in the cleft. D was 0.25 μm^2/ms. (A) Uptake K_m values were 2 and 200 μM for neuronal and glial uptake. (B) Uptake K_m values were increased to 20 and 1000 μM.

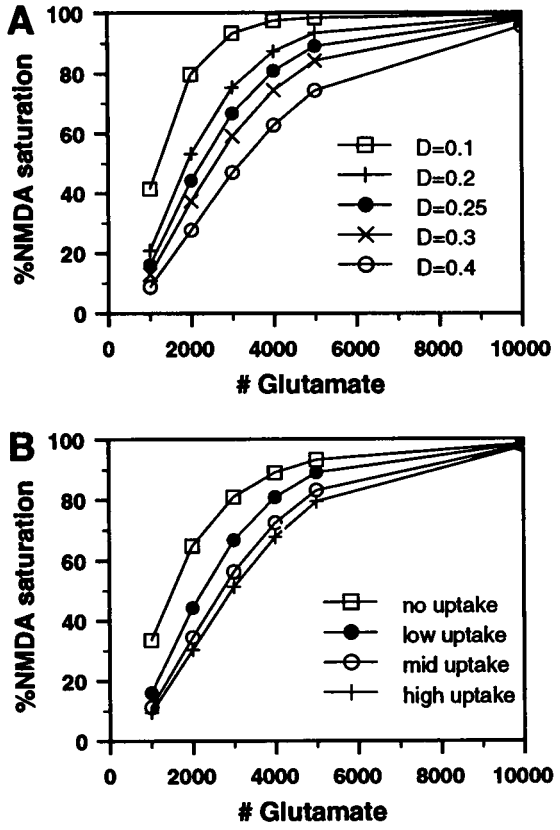

FIGURE 6 Percentage saturation of NMDA receptors by single vesicles of glutamate. Saturation was measured as the number of receptors in the double bound state + the number double bound desensitized + the number in the open state with the sum divided by the total number of receptors. Plotted is the maximum saturation value reached over time, expressed as a percentage. (A) Percentage NMDA receptor saturation for different diffusion coefficient values. (B) Percentage saturation for different uptake capacity values. K_m values were 2 and 200 μM for neuronal and glial uptake, respectively. As noted in the text, increasing these values to 20 and 1000 μM had little effect on the plotted values. The filled circles are for D = 0.25 μm^2/ms and low uptake capacity in both plots.

tamate molecules bound, including those in the open channel and desensitized states.

Single vesicles of glutamate did not saturate NMDA receptors unless the diffusion coefficient was small and the amount of transmitter released from a vesicle was large. Fig. 6 A shows that even when D was 0.1 μm^2/ms, NMDA receptors did not become 90% saturated until the number of glutamate molecules in a vesicle was 3000. When D was 0.2 μm^2/ms, 5000 glutamate molecules were needed to get 90% NMDA receptor saturation. When 10,000 glutamate molecules were in a vesicle, NMDA receptors were more than 90% saturated regardless of the value of the diffusion coefficient used in the model. For the range of glutamate molecules thought to exist in a vesicle (1000–4000) and the value of D considered most likely (D = 0.25 μm^2/ms), NMDA receptor saturation ranged from 16% to 81%, implying that NMDA receptors are not saturated by a single vesicle of glutamate.

The extent of NMDA receptor saturation was not dependent on receptor density because in all cases modeled the number of receptors was much smaller than the number of transmitter molecules released. The results in Fig. 6 A varied by up to 2% for the different receptor densities modeled.

The extent of NMDA receptor saturation was dependent on uptake capacity, but only a small effect was found by reducing uptake affinity. Fig. 6 B compares percentage saturation for no uptake and three different levels of uptake when D was 0.25 μm^2/ms. Uptake capacity had its largest effect on saturation when the number of transmitter molecules released was 2000–4000. Increasing the uptake affinity K_m values from 2 and 200 μM to 20 and 1000 μM increased saturation levels slightly, but differences were hard to distinguish from those shown in Fig. 6 B and are not shown.

Non-NMDA receptors also were not saturated unless D was small and the amount of transmitter in a vesicle was large. As shown in Fig. 7, percentage saturation was similar to that found for NMDA receptors except that the slope of the increase with increasing numbers of glutamate molecules in a vesicle was less steep. Non-NMDA receptor saturation was much smaller in simulations that used the Raman and Trussell (1995) kinetic scheme and parameter values or the Jonas et al. (1993) parameter values without compensation for temperature. For the assumed usual case

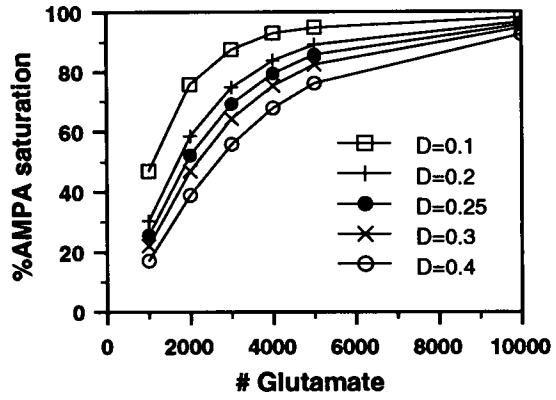

FIGURE 7 Percentage saturation of non-NMDA receptors by single vesicles of glutamate for different diffusion coefficient values.

of $D = 0.25\ \mu m^2/ms$, 3000 glutamate molecules in a vesicle and low uptake capacity, percentage saturation was 69% with the temperature-compensated Jonas et al. (1993) values, 49% without the temperature compensation, and 20% with the Raman and Trussell (1995) kinetic scheme and parameter values.

Unlike NMDA receptor saturation, non-NMDA receptor saturation was not significantly affected by different modeled uptake capacity values. This was also true when the parameter values without temperature compensation were used. However, in simulations with the Raman and Trussell (1995) kinetics, percentage saturation was reduced in the low uptake capacity case compared to the no uptake case, but further increases in uptake capacity produced only minor changes. Reducing uptake affinity K_m values to 200 and 1000 μM had a negligible effect on the percentage saturation values for all of the kinetic schemes and parameter values tested.

The role of glutamate uptake in shaping the amplitude and decay of the NMDA and non-NMDA response

Glutamate uptake played a significant role in determining the amplitude of the NMDA response. Fig. 8 *A* shows the peak number of channels in the open state for three uptake capacities as a percentage of the peak number when there was no uptake. For the low uptake capacity, the peak number of open NMDA receptor channels was reduced by 10–50%, depending on the number of glutamate molecules in a vesicle. This large effect on amplitude occurred because uptake removed a significant amount of glutamate before the binding reaction kinetics would allow the peak number of open channels to be reached.

The time course of the decay of the NMDA response was the same for all uptake capacities tested, but decay was slightly longer when there was no uptake. Fig. 8 *B* shows the decay of the log of the number of open NMDA channels over time when there was no uptake or three different uptake capacities. The slopes of the curves for the three

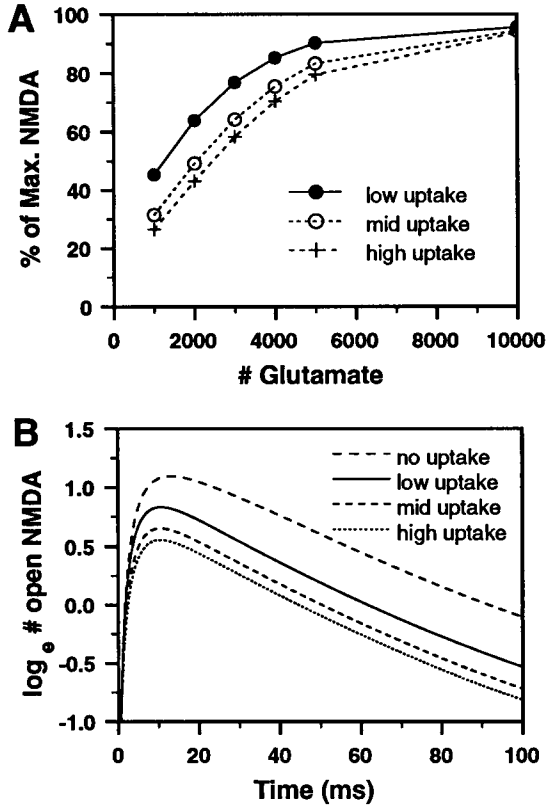

FIGURE 8 Effect of uptake on the amplitude and time course of the NMDA response. (*A*) Peak response amplitude (peak number of open channels) is given as a percentage of the peak response amplitude when there was no uptake. (*B*) Time course of the response is shown as the $\log_e$ of the number of open NMDA channels.

uptake capacities were the same, but the slope for the no uptake curve was less steep for the first 50–60 ms. Beyond 60 ms the decay was identical for all of the curves. When uptake was present, glutamate concentration dropped below 1 μM by 2.0 ms, and consequently, the decay rate depended only on unbinding kinetics. However, when there was no uptake, glutamate concentration was still 5–10 μM at 10 ms and binding of glutamate to NMDA receptors could still occur; only after 60 ms did the decay depend only on unbinding kinetics.

In contrast, glutamate uptake had only a small effect on the amplitude of the non-NMDA response. As shown in Fig. 9 *A*, the low uptake capacity that caused a 10–50% reduction in the NMDA response amplitude compared to the no uptake case caused less than a 5% reduction in the peak number of open non-NMDA receptor channels. The reason for this was that the peak number of open non-NMDA channels occurred at about 0.3 ms, but as shown in Fig. 5 *A*, uptake did not even begin to affect the concentration of glutamate in the cleft until about 0.2 ms. Consequently, the effect on the response amplitude was small. These results suggest that glutamate uptake blockers should selectively affect the amplitude of the NMDA receptor mediated response to stimuli while having almost no effect on the amplitude of the non-NMDA receptor mediated response.

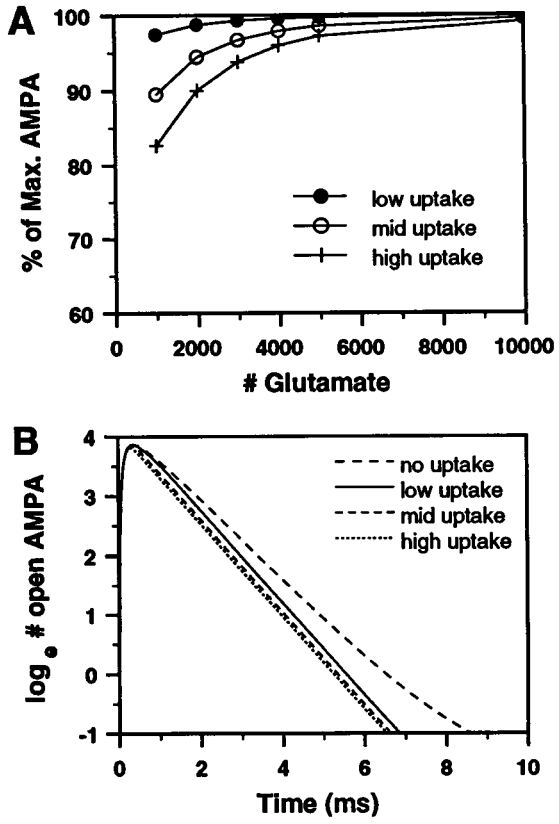

FIGURE 9 Effect of uptake on the amplitude and time course of the non-NMDA response. (*A*) Peak response amplitude (peak number of open channels) is given as a percentage of the peak response amplitude when there was no uptake. Note that the scale is different from that in Fig. 8 *A*. (*B*) Time course of the response is shown as the $\log_e$ of the number of open channels.

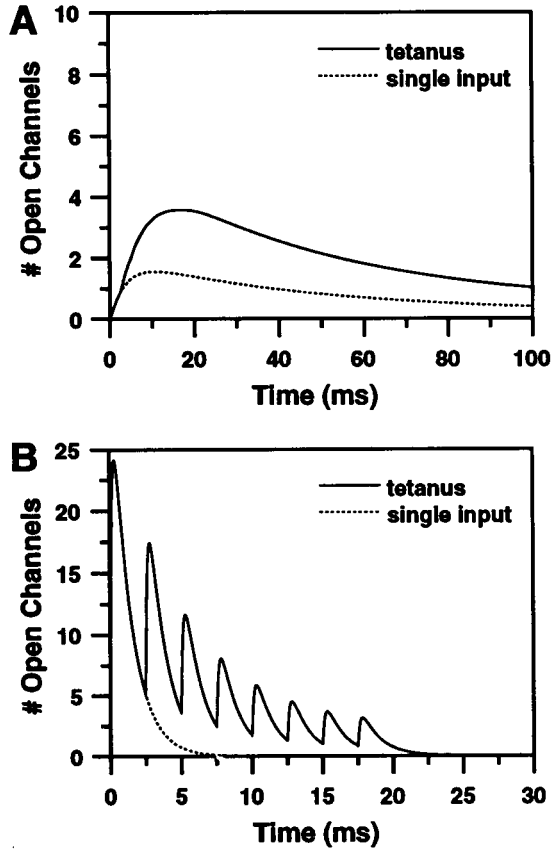

FIGURE 10 Effect of a tetanus on the number of non-NMDA and NMDA channels reaching the open state (no magnesium block). (*A*) NMDA. (*B*) Non-NMDA.

As with the NMDA response, the time course of the decay of the non-NMDA response was the same for all uptake capacities tested, but was increased when there was no uptake (Fig. 9 *B*). When uptake was present, glutamate disappeared from the cleft shortly after the peak of the non-NMDA response, and there was no rebinding of transmitter to receptors to slow the rate of decay. However, when uptake was eliminated, enough glutamate was present in the cleft to allow further binding to non-NMDA receptors (i.e., glutamate concentration was still 40 μM at 2.0 ms).

Receptor saturation with tetanic stimulation

When glutamate release was modeled to occur as a 400-Hz, 8-pulse tetanus (assuming a release probability of 1.0), NMDA receptors were >90% saturated for all parameter combinations tested (a 200-Hz, 4-pulse tetanus also caused >90% NMDA receptor saturation). The tetanus significantly increased the peak number of open NMDA receptor channels, as shown in Fig. 10 *A*. As expected, the increase in the number of open NMDA channels was smallest in those cases where single inputs caused >90% saturation of NMDA receptors (i.e., $D = 0.1$ μm^2/ms and large numbers of glutamate molecules in a vesicle) and largest in those cases where single pulses caused the least saturation.

Although the 400-Hz, 8-pulse tetanus increased the percentage saturation of non-NMDA receptors compared to release of a single vesicle, the percentage saturation did not exceed 90% for all conditions tested, as it did for NMDA receptors. After release of the first vesicle, many receptors entered the single bound desensitized state, and although some moved to the double bound desensitized state with the tetanus, the number was not usually enough to bring the saturation percentage above 90% (except for those cases when saturation was close to or above 90% after release of the first vesicle).

More significant is the fact that the peak number of open non-NMDA receptor channels fell precipitously with subsequent pulses in the tetanus because of receptor desensitization (Fig. 10 *B*). In simulations with the Jonas et al. (1993) parameter values without temperature compensation or with the Raman and Trussell (1995) non-NMDA reaction scheme and parameter values, the last pulse in the tetanus also caused a response whose amplitude was less than 25% of that for the first pulse.

Response in a model of a dentate granule cell

Synaptic conductances were determined by multiplying the number of open NMDA and non-NMDA channels computed with the model by a single channel conductance (8 pS for non-NMDA, 50 pS for NMDA). These conductances were used in a model of a dentate granule cell that included complete morphology obtained from serial reconstructions (Holmes and Levy, 1990). Responses to single input and tetanic input at either 1 or 108 medial perforant path synapses were computed.

In these simulations the number of glutamate molecules in a vesicle was 2000 and the non-NMDA receptor density was 2000/μm^2. The use of 3000 for both of these parameters caused EPSPs that were much larger than the 100–200-μV amplitude estimated for unitary EPSPs in dentate granule cells (McNaughton et al., 1981) or CA1 pyramidal cells (Sayer et al., 1990). (The same was true when the Jonas et al. (1993) non-NMDA kinetic parameter values without temperature compensation were used).

Fig. 11 shows the voltage response at the soma due to input at a single medial perforant path synapse (located in the middle of the dendritic tree). The NMDA and non-NMDA receptor mediated components of the EPSP are shown. The NMDA receptor mediated component was a much larger part of the EPSP than is typically reported, even though 1.2 mM extracellular magnesium was included in the model and the voltage change at the synapse was less than 2 mV. One possible explanation is that the number of NMDA receptors was so small that channel openings at a single synapse should be computed stochastically rather than deterministically. Because of magnesium block, the peak NMDA conductance that produced the voltage response in Fig. 11 was 2 pS, or less than 5% of the single channel conductance! With a stochastic simulation, the conductance would bounce between 0 and 50 pS, and this could produce much different voltage responses. Fig. 11 can be interpreted as an average of many such stochastic simulations. One would expect the variability among individual stochastic simulations to be extremely large.

When the stimulation was strong (108 synapses activated), the NMDA conductance was much larger with tetanic stimulation than with single stimulation (Fig. 12 *A*). The strong input caused the cell to fire action potentials, which propagated back up the dendrites and produced spikes in the conductance plots. With the parameter values used in these simulations, single vesicles of glutamate caused 45% saturation of NMDA receptors, but tetanic input caused more than 98% saturation. Thus, part of the increase in conductance with the tetanus was due to increased binding of glutamate to NMDA receptors and part was due to relief of voltage-dependent magnesium block of NMDA receptor channels.

To get a rough estimate of how much of the increased conductance was due to increased glutamate binding to NMDA receptors, the simulations leading to Fig. 12 *A* were repeated, but with the number of glutamate molecules in a vesicle set to 10,000 to cause saturation of NMDA receptors

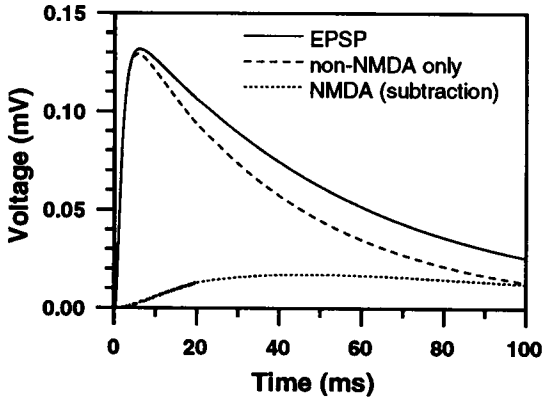

FIGURE 11 EPSP observed at the soma due to activation of a single medial perforant path synapse in a dentate granule cell model. Components due to NMDA and non-NMDA receptor activation are shown. Magnesium concentration was 1.2 mM. Parameter values used were D = 0.25 μm^2/ms, 2000 glutamate molecules in a vesicle, NMDA and non-NMDA densities of 600 and 2,000/μm^2, respectively, and high-affinity, low-capacity uptake.

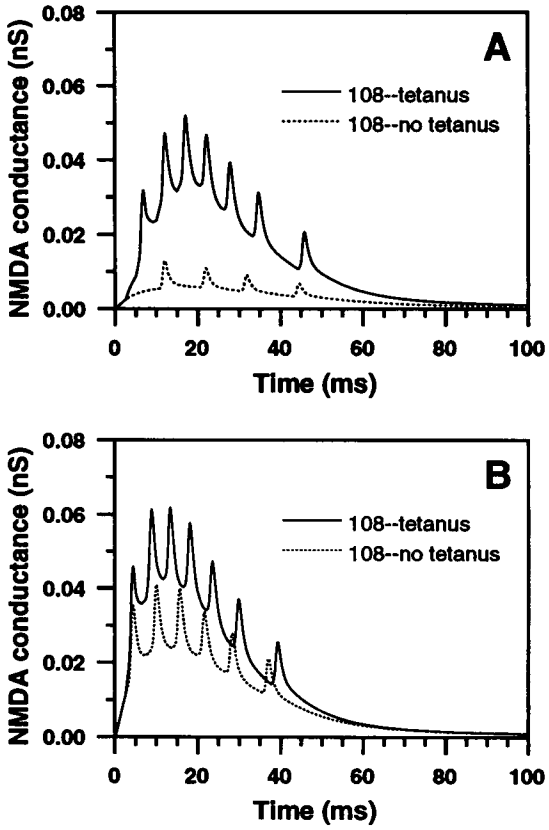

FIGURE 12 NMDA conductance at a synapse for single or tetanic co-activation of 108 synapses. Tetanus was 8 pulses at 400 Hz. (*A*) Conductances computed with D = 0.25 μm^2/ms, 2000 glutamate in a vesicle, NMDA and non-NMDA densities of 600 and 2,000/μm^2, and high-affinity, low-capacity uptake. (*B*) Conductances computed with the same parameters except that 10,000 glutamate molecules were in the vesicle.

with single vesicle release. In this case (Fig. 12 *B*) the tetanus could not effect much additional binding to NMDA receptors, and most of the increase in conductance was due to relief of voltage dependent magnesium block of NMDA receptors.

If it can be assumed that the increase in conductance due to increased glutamate binding can be approximated by the difference between the lower curves in Fig. 12, *A* and *B*, and the increase in conductance due to relief of magnesium block can be approximated by the difference between the lower curve in Fig. 12 *B* and either of the upper curves, then it is possible to estimate the relative size of the increase in calcium influx due to increased glutamate binding. Calcium influx was computed from the calcium component of the current through NMDA receptor channels at a synapse for the four cases given in Fig. 12. With the above assumptions, it was found that about two-thirds of the increase in calcium influx with a tetanus came from increased glutamate binding to NMDA receptors and about one-third came from the relief of voltage-dependent magnesium block. The NMDA conductance for the non-tetanic input when vesicle content was 10,000 generated approximately 2.8 times as much calcium influx as when vesicle content was 2000. Calcium influx for tetanic input was approximately 1.3 times that found for non-tetanic input when vesicle content was 10,000. (Calcium influx differed by only 10% for a tetanus whether vesicle content was 2000 or 10,000, as might be expected, because receptors were saturated in both cases.) This method of separating the effects of increased glutamate binding and relief of voltage-dependent channel block on calcium influx is far from exact, but it does suggest that both factors play significant roles.

DISCUSSION

Time course of glutamate in the cleft

The simulation results, in agreement with previous theoretical and experimental studies (Eccles and Jaeger, 1958; Barbour et al., 1994; Clements et al., 1992), indicate that the time course of glutamate in the cleft is brief. How brief depends on diffusion and uptake. Clements et al. (1992) suggest that peak glutamate concentration is 1.1 mM and that glutamate concentration is >1 mM for <100–200 μs, >100 μM for >1 ms, and >50 μM for less than 5 ms. The results here are in close quantitative agreement with the Clements et al. (1992) results when uptake is excluded from the model. However, when a low level of uptake was modeled, glutamate concentration was >1 mM for <100 μs, >100 μM for 600 μs, and >50 μM for only 0.9 ms. This difference might be explained if the "low" uptake level used in the simulations actually represents a level much higher than is actually present—we do not know the density of transporters in neuronal or glial membrane. This "low" uptake level may be much higher than that present in the Clements et al. (1992) preparation. A smaller diffusion coefficient would also prolong the time of glutamate in the cleft, but even when D was 0.1 μm^2/ms uptake still caused glutamate concentration to drop below 50 μM by 1.5 ms.

Single vesicles of glutamate do not saturate NMDA and non-NMDA receptors

The calculations given here suggest that NMDA receptors are only 60–70% saturated by single vesicles of glutamate. This is far less than the 97% computed by Clements et al. (1992). Percentage saturation is sensitive to the glutamate diffusion coefficient, the amount of transmitter released by a vesicle, and to a lesser extent, the degree of uptake. NMDA receptors do not become saturated unless the diffusion coefficient is small and the number of transmitter molecules released in a vesicle is large. It seems that the synapse operates in a range where a change in the ability of glutamate to diffuse or a change in the number of transmitter molecules released in a vesicle can have a large effect on the extent of receptor saturation. The results here suggest that if two or more vesicles of glutamate are released at a synapse, then saturation of NMDA receptors would be highly likely. High-frequency tetanic input always saturated NMDA receptors.

Non-NMDA receptors were less than 90% saturated by single vesicles of glutamate in almost all of the simulations, and with the parameter values most consistent with experimental data, non-NMDA receptors were 69% saturated. This number is consistent with some of the calculations made by Jonas et al. (1993). Much lower saturation levels were obtained with the Raman and Trussell (1992, 1995) AMPA kinetic scheme and parameter values or the Jonas et al. (1993) parameter values (as given, without the temperature compensation factor).

These results are in contrast to those of Tong and Jahr (1994a) and Tang et al. (1994), who suggest that AMPA receptors are saturated by single vesicles of glutamate. The Tong and Jahr (1994a) saturation result was based on studies that used a 0.9 ms pulse of 1 mM glutamate, but they also showed that a 0.3 ms pulse did not cause saturation. The time course of glutamate in the cleft computed here is much closer to that of a 0.3-ms glutamate pulse than a 0.9-ms pulse. The Tang et al. (1994) result was based on the fact that when desensitization is blocked by cyclothiazide, temporal summation of mEPSCs is nonlinear and the absolute amplitude of the second mEPSC is not much higher than that of the first mEPSC. However, this is not a very sensitive measure of saturation. If desensitization is removed from the present model, temporal summation of mEPSCs is nonlinear even with 50% saturation and the absolute amplitude of the second mEPSC is only 10–15% higher than the first.

Non-NMDA receptor saturation did increase with a tetanus, but the number of channels becoming open did not increase with each pulse of the tetanus because of the receptor binding kinetics and desensitization (Trussell et al., 1993). In fact, the peak number of open channels decreased

sharply during the tetanus to the point where the last of the eight pulses produced a response that was less than 20% of that for the first pulse. It is not likely that the probability of release will be 1.0 for each of the eight pulses, but even when the probability of release was 0.5, the desensitization caused a major reduction in the response amplitude with successive pulses in the train.

Choices of parameter values

Although the parameter values used in this study were chosen to be consistent with experimental data, actual values for some parameters might be different. The range of values for the diffusion coefficient used here covers well the expected value of D given its value in aqueous solution and the expected reduction due to tortuosity (Rice et al., 1985; Nicholson and Phillips, 1981). However, it was recently suggested that the extracellular volume around dendritic spines might limit diffusion more than currently believed and cause glutamate to remain at high concentrations in the synaptic cleft (Barbour et al., 1994). If D were to be reduced much below 0.1 μm^2/ms then NMDA and non-NMDA receptors could be saturated with the release of single vesicles.

Only one set of NMDA receptor kinetic data was used in the present model, and this set of parameter values was a hybrid of values reported in the literature. It is possible that faster kinetics, taking into account temperature effects, would have been more appropriate. Although faster kinetics might lead to greater saturation with single vesicles of glutamate, this does not mean that a tetanus would be unable to recruit more receptors to the open state. Without a tetanus the faster unbinding rate could take receptors away from the double bound state before channel opening could occur. With a tetanus, the time near saturation would be increased, thereby increasing the probability of moving to the open state.

The non-NMDA receptor kinetic scheme used here was that given by Jonas et al. (1993), with the rate constants doubled as a first approximation to compensate for temperature. Without this compensation, the peak number of open channels due to activation of a single synapse was about half as large, but the slower time course gave an EPSP that was again similar to that which single synapses are thought to produce (McNaughton et al., 1981; Sayer et al., 1990). Conversely, use of the Raman and Trussell (1992, 1995) kinetic scheme gave EPSPs that were too small.

Effect of uptake on the NMDA and non-NMDA response

The effect of glutamate uptake on the amplitude and time course of NMDA and non-NMDA receptor mediated responses has been studied experimentally with mixed results. Uptake blockers have been found to reduce (Mennerick and Zorumski, 1994), to increase (Tong and Jahr, 1994b), or not to affect (Isaacson and Nicoll, 1993; Sarantis et al. 1993) (Mennerick and Zorumski, 1994) non-NMDA synaptic current amplitude while either prolonging or having no effect on the decay time course. Uptake blockers have been found to reduce (Sarantis et al., 1993) or have no effect on NMDA synaptic current amplitude. Also, different results have been obtained at different temperatures (Tong and Jahr, 1994b). It is not clear why the experimental results have been so different, but one explanation could be the different methods of applying and clearing glutamate.

In the present simulations uptake blockers had a negligible effect on non-NMDA receptor mediated response amplitude and caused a small but significant prolongation of the decay time course. The amplitude is determined by the transmitter concentration in the first 300–400 μs after release because of the binding kinetics. During this time, transmitter concentration is falling rapidly because of diffusion, and uptake blockers do not appreciably affect the concentration before 200 μs. Uptake blockers do affect glutamate concentration after the first 500 μs, but by then the peak amplitude of the non-NMDA response has passed. The decay time course of the non-NMDA response is slowed slightly when uptake is blocked, but the effect is small because after the first 500 μs glutamate concentration is below the equilibrium constant for non-NMDA receptor binding. This small difference might disappear altogether with larger diffusion coefficient values such as those near the value in aqueous solution.

The simulations suggest that uptake blockers should increase the amplitude of the NMDA response by 10–50% while having little or no effect on the decay time course. Because the peak NMDA response occurs so much later and the equilibrium constant is so much smaller than for non-NMDA receptors, the increased glutamate concentration in the cleft after the first 500 μs due to uptake blockers can have a strong effect on the response amplitude. The decay time course was not affected because of the slow binding and unbinding kinetics of NMDA receptors and the fact that glutamate concentration in the cleft drops to very low levels shortly after the peak of the NMDA response, even when uptake is blocked.

The large NMDA response in the dentate cell model

The NMDA conductance predicted with this model gave an NMDA component of the EPSP (voltage measured at the soma; synapse in the middle of the dendritic tree) that was far larger than that observed experimentally (Lambert and Jones, 1989) and a calcium influx through NMDA receptor channels that was nearly double that in our previous model (Holmes and Levy, 1990). The large response occurred despite the fact that only 2–4 NMDA channels were open at a synapse at the peak of the response, and these were largely blocked by magnesium. Four open NMDA channels at the peak of the response is consistent with estimates of Silver

et al. (1992) and Bekkers and Stevens (1989). The response could be made smaller if the simulated receptor density were smaller, but the density used most often was the equivalent of having only 19 NMDA channels at the synapse. To reduce the response three- to fourfold would mean that there are fewer than six NMDA channels at a synapse with only one open at the peak of the response. This number seems much too small, although single NMDA receptor channel openings have been observed as part of an EPSC (Silver et al., 1992).

There are a number of possible ways to explain the large response. First, if kinetics were faster (because of a higher temperature) the NMDA conductance time course would be faster and the NMDA response would be smaller. This possibility cannot be ruled out. Second, given the small numbers of channels involved, a stochastic simulation might be more appropriate (Faber et al., 1992; Bartol et al., 1991). However, the results here would still represent an average of a large number of stochastic simulations. A small NMDA response would occur in many simulations, but a large response would also be found. Such large NMDA responses have not been reported to date. Third, a significant number of channels may be in a long-lasting desensitized state. The number of channels that could become open would be reduced significantly if 50% of the receptors were desensitized. Finally, it is possible that the NMDA binding reaction may exhibit a glycine dependence that is more restrictive than currently believed. These are considerations that await further study.

Implications for long-term potentiation

The lack of saturation of NMDA receptors by single vesicles of glutamate means that tetanic input will increase calcium influx through NMDA receptor channels by two mechanisms: the recruitment of new receptors to the double bound state and the relief of voltage-dependent magnesium block. If single vesicles of glutamate saturated NMDA receptors, then subsequent pulses of a tetanus would bring no more NMDA receptors to the double bound state. An important source of nonlinearity of calcium influx through NMDA receptor channels would be lost, as the sole effect of a tetanus on calcium influx would be through relief of magnesium block. The calculations here suggest that a significant amount of the increase in calcium influx through NMDA receptor channels is due to the recruitment of new receptors to the double bound state. Whether or not NMDA receptors are saturated by single vesicles of glutamate makes only a small difference on the calcium influx caused by a tetanus. However, for non-tetanic input (single pulse), calcium influx is much higher when NMDA receptors are saturated by single vesicles of glutamate than when they are not.

The lack of saturation of NMDA and non-NMDA receptors has some implications for the use of quantal analysis to determine the mechanism involved in LTP. There has been some debate as to whether the change with LTP is due to an increase in quantal content or quantal size. The results shown here suggest that an increase in quantal content, by increasing the fraction of receptors that are activated, might look very much like an increase in quantal size. Thus, if the change with LTP is due to an increase in the likelihood of multivesicular release (Tong and Jahr, 1994a), the percentage receptor saturation would increase, and the result would be similar to that expected for an increase in quantal size.

I would like to thank G. M. Zulfakir Ali for programming the ADI method in the two-dimensional model and Donald M. Weekley for programming the various AMPA receptor schemes.

This work was supported by National Institute of Mental Health grant MH51081.

REFERENCES

Balcar, V. J., and G. A. R. Johnston. 1972a. The structural specificity of the high affinity uptake of L-glutamate and L-aspartate by rat brain slices. *J. Neurochem.* 19:2657–2666.

Balcar, V. J., and G. A. R. Johnston. 1972b. Glutamate uptake by brain slices and its relation to the depolarization of neurones by acidic amino acids. *J. Neurobiol.* 3:295–301.

Barbour, B., B. U. Keller, I. Llano, and A. Marty. 1994. Prolonged presence of glutamate during excitatory synaptic transmission to cerebellar Purkinje cells. *Neuron.* 12:1331–1343.

Bartol, T. M., B. R. Land, E. E. Salpeter, and M. M. Salpeter. 1991. Monte Carlo simulation of miniature end-plate current generation in the vertebrate neuromuscular junction. *Biophys. J.* 59:1290–1307.

Baudry, M., and J. L. Davis, eds. 1991. Long-Term Potentiation: A Debate of Current Issues. MIT Press, Cambridge, MA.

Baudry, M., and J. L. Davis, eds. 1994. Long-Term Potentiation, Vol. 2. MIT Press, Cambridge, MA.

Bekkers, J. M., and C. F. Stevens. 1989. NMDA and non-NMDA receptors are co-localized at individual excitatory synapses in cultured rat hippocampus. *Nature.* 341:230–233.

Burger, P. M., E. Mehl, P. L. Cameron, P. R. Maycox, M. Baumert, F. Lottspeich, P. DeCamilli, and R. Jahn. 1989. Synaptic vesicles immunoisolated from rat cerebral cortex contain high levels of glutamate. *Neuron.* 3:715–720.

Clements, J. D., R. A. J. Lester, G. Tong, C. E. Jahr, and G. L. Westbrook. 1992. The time course of glutamate in the synaptic cleft. *Science.* 258:1498–1501.

Clements, J. D., and G. L. Westbrook. 1991. Activation kinetics reveal the number of glutamate and glycine binding sites on the N-methyl-D-aspartate receptor. *Neuron.* 7:605–613.

Desmond, N. L., and W. B. Levy. 1986. Changes in the postsynaptic density with long-term potentiation in the dentate gyrus. *J. Comp. Neurol.* 253:476–482.

Eccles, J. C., and J. C. Jaeger. 1958. The relationship between the mode of operation and the dimensions of the junctional regions at synapses and motor end-organs. *Proc. R. Soc. Lond. [Biol.].* 148:38–56.

Edmonds, B., and D. Colquhoun. 1992. Rapid decay of averaged single-channel NMDA receptor activations recorded at low agonist concentration. *Proc. R. Soc. Lond. [Biol.].* 250:279–286.

Faber, D. S., W. S. Young, P. Legendre, and H. Korn. 1992. Intrinsic quantal variability due to stochastic properties of receptor-transmitter interactions. *Science.* 258:1494–1498.

Garthwaite, J. 1985. Cellular uptake disguises action of L-glutamate on N-methyl-D-aspartate receptors. *Br. J. Pharmacol.* 85:297–307.

Gerald, C. F., and P. O. Wheatley. 1994. Applied Numerical Analysis. Addison-Wesley Publishing Company, Reading, MA.

Harris, K. M., and D. M. D. Landis. 1986. Membrane structure at synaptic junctions in area CA1 of the rat hippocampus. *Neuroscience.* 19: 857–872.

Hertz, L. 1979. Functional interactions between neurons and astrocytes. I. Turnover and metabolism of putative amino acid transmitters. *Prog. Neurobiol.* 13:277–323.

Hertz, L., A. Schousboe, N. Boechler, S. Mukerji, and S. Fedoroff. 1978. Kinetic characteristics of the glutamate uptake into normal astrocytes in cultures. *Neurochem. Res.* 3:1–14.

Holmes, W. R., and W. B. Levy. 1990. Insights into associative long-term potentiation from computational models of NMDA receptor-mediated calcium influx and intracellular calcium concentration changes. *J. Neurophysiol.* 63:1148–1168.

Isaacson, J. S., and R. A. Nicoll. 1993. The uptake inhibitor L-trans-PDC enhances responses to glutamate but fails to alter the kinetics of excitatory synaptic currents in the hippocampus. *J. Neurophysiol.* 70: 2187–2191.

Jonas, P., G. Major, and B. Sakmann. 1993. Quantal components of unitary EPSCs at the mossy fibre synapse on CA3 pyramidal cells of rat hippocampus. *J. Physiol. (Lond.).* 472:615–663.

Lambert, J. D. C., and R. S. G. Jones. 1989. Activation of N-methyl-D-aspartate receptors contributes to the EPSP at perforant path synapses in the rat dentate gyrus in vitro. *Neurosci. Lett.* 97:323–328.

Lester, R. A. J., J. D. Clements, G. L. Westbrook, and C. E. Jahr. 1990. Channel kinetics determine the time course of NMDA receptor-mediated synaptic currents. *Nature.* 346:565–567.

Lester, R. A. J., and C. E. Jahr. 1992. NMDA channel behavior depends on agonist affinity. *J. Neurosci.* 12:635–643.

Lester, R. A. J., G. Tong, and C. E. Jahr. 1993. Interactions between the glycine and glutamate binding sites of the NMDA receptor. *J. Neurosci.* 13:1088–1096.

Lin, F., and C. F. Stevens. 1994. Both open and closed NMDA receptor channels desensitize. *J. Neurosci.* 14:2153–2160.

Lisman, J. 1989. A mechanism for the Hebb and the anti-Hebb processes underlying learning and memory. *Proc. Natl. Acad. Sci. USA.* 86: 9574–9578.

Longsworth, L. G. 1953. Diffusion measurements at 25°, of aqueous solutions of amino acids, peptides and sugars. *J. Am. Chem. Soc.* 75:5705–5709.

Mascagni, M.V. 1989. Numerical methods for neuronal modeling. *In* Methods in Neuronal Modeling. C. Koch and I. Segev, editors. MIT Press, Cambridge, MA. 439–484.

McNaughton, B. L., C. A. Barnes, and P. Andersen. 1981. Synaptic efficacy and EPSP summation in granule cells of rat fascia dentata studied in vitro. *J. Neurophysiol.* 46:952–966.

Mennerick, S., and C. F. Zorumski. 1994. Glial contributions to excitatory neurotransmission in cultured hippocampal cells. *Nature.* 368:59–62.

Nicholson, C., and J. M. Phillips. 1981. Ion diffusion modified by tortuosity and volume fraction in the extracellular microenvironment of the rat cerebellum. *J. Physiol. (Lond.).* 321:225–257.

Patneau, D. K., M. L. Mayer, D. E. Jane, and J. C. Watkins. 1992. Activation and desensitization of AMPA/kainate receptors by novel derivatives of willardine. *J. Neurosci.* 12:595–606.

Raman, I. M., and L. O. Trussell. 1992. The kinetics of the response to glutamate and kainate in neurons of the avian cochlear nucleus. *Neuron.* 9:173–186.

Raman, I. M., and L. O. Trussell. 1995. The mechanism of α-amino-3-hydroxy-5-methyl-4-isoxazolepropionate receptor desensitization after removal of glutamate. *Biophys. J.* 68:137–146.

Rice, M. E., G. A. Gerhardt, P. M. Hierl, G. Nagy, and R. N. Adams. 1985. Diffusion coefficients of neurotransmitters and their metabolites in brain extracellular fluid space. *Neuroscience.* 3:891–902.

Riveros, N., J. Fiedler, N. Lagos, C. Munoz, and F. Orrego. 1986. Glutamate in rat brain cortex synaptic vesicles: influence of the vesicle isolation procedure. *Brain Res.* 386:405–408.

Sarantis, M., L. Ballerini, B. Miller, R. A. Silver, M. Edwards, and D. Attwell. 1993. Glutamate uptake from the synaptic cleft does not shape the decay of the non-NMDA component of the synaptic current. *Neuron.* 11:541–549.

Sayer, R. J., M. J. Friedlander, and S. J. Redman. 1990. The time course and amplitude of EPSPs evoked at synapses between pairs of CA3/CA1 neurons in the hippocampal slice. *J. Neurosci.* 10:826–836.

Schousboe, A. 1981. Transport and metabolism of glutamate and GABA in neurons and glial cells. *Int. Rev. Neurobiol.* 22:1–45.

Silver, R. A., S. F. Traynelis, and S. G. Cull-Candy. 1992. Rapid-time course miniature and evoked excitatory currents at cerebellar synapses in situ. *Nature.* 355:163–166.

Storm-Mathisen, J. 1977. Glutamic acid and excitatory nerve endings: reduction of glutamic acid uptake after axotomy. *Brain Res.* 120: 379–386.

Tang, C-M., M. Margulis, Q-Y Shi, and A. Fielding. 1994. Saturation of postsynaptic glutamate receptors after quantal release of transmitter. *Neuron.* 13:1385–1393.

Tong, G., and C. E. Jahr. 1994a. Multivesicular release from excitatory synapses of cultured hippocampal neurons. *Neuron.* 12:51–59.

Tong, G., and C. E. Jahr. 1994b. Block of glutamate transporters potentiates postsynaptic excitation. *Neuron.* 13:1195–1203.

Trussell, L. O., S. Zhang, and I. M. Raman. 1993. Desensitization of AMPA receptors upon multiquantal neurotransmitter release. *Neuron.* 10:1185–1196.

Vyklicky, L., Jr., D. K. Patneau, and M. L. Mayer. 1991. Modulation of excitatory synaptic transmission by drugs that reduce desensitization at AMPA/kainate receptors. *Neuron.* 7:971–984.

Wathey, J. C., M. M. Nass, and H. A. Lester. 1979. Numerical reconstruction of the quantal event at nicotinic synapses. *Biophys. J.* 27:145–164.